Chemistry & Biodiversity

WILEY-VCH

CHEMISTRY & BIODIVERSITY

RESEARCH ARTICLE

Iboga-Indole Alkaloids as Potential Plasmodial Inhibitors: Identification, Biosynthesis, and Molecular Docking Studies

Smith B. Babiaka[1,2] | Methodius S. Lahngong[3] | Conrad V. Simoben[4] | Dennis S. B. Ongarora[5] | Godloves F. Chi[1] | Dieudonné T. Tshitenge[6] | Rajshekhar Karpoormath[7] | Marwaan Rylands[8] | James A. Mbah[1] | Kennedy O. Abuga[5] | E. Joel Loveridge[9] | Michel Frédérich[3]

[1]Department of Chemistry, Faculty of Science, University of Buea, Buea, Cameroon | [2]Department of Microbial Bioactive Compounds, Interfaculty Institute for Microbiology and Infection Medicine, University of Tübingen, Tübingen, Germany | [3]Pharmacognosy Laboratory, Center For Interdisciplinary Research On Medicine (CIRM), ULiége, Liège, Belgium | [4]Structural Genomics Consortium, University of Toronto, Toronto, Canada | [5]Department of Pharmaceutical Chemistry, Pharmaceutics and Pharmacognosy, Faculty of Health Sciences, University of Nairobi, Nairobi, Kenya | [6]Small Molecules, R&D Crop Science, Monheim am Rhein, Germany | [7]Department of Pharmaceutical Chemistry, University of KwaZulu-Natal, Durban, South Africa | [8]Department of Chemistry, University of Cape Town, Cape Town, South Africa | [9]Department of Chemistry, Swansea University, Swansea, UK

Correspondence: Smith B. Babiaka (babiaka.smith@ubuea.cm) | Dieudonné T. Tshitenge (dtshitenge2007@yahoo.com)

Received: 24 April 2025 | **Revised:** 23 September 2025 | **Accepted:** 24 September 2025

Funding: The research was funded by the Alexander von Humboldt Foundation for Georg Forster and Georg Forster-Bayer Research fellowships (Ref. 3.4–CMR–1220727–GF-P) at the University of Tübingen, Germany.

Keywords: antiplasmodial activity | biogenetic pathway | iboga alkaloids | protein-ligand co-folding | voacamine | *Voacanga africana* | voacorine

ABSTRACT

A previously undescribed iboga-indole alkaloid, voacamine A (**1**), and the known alkaloids, voacamine (**2**), voacorine (**3**), and voacangine (**4**) were isolated from the stem bark of *Voacanga africana*. The structures of the alkaloids were established by one- and two-dimensional nuclear magnetic resonance analyses as well as by comparison with published data. The antiplasmodial activity of the alkaloids was assessed on a chloroquine-sensitive 3D7 *Plasmodium falciparum* (*Pf3D7*) strain, and the half-maximal inhibitory concentration (IC_{50}) values were determined. Alkaloids **2** and **3** showed good in vitro antiplasmodial activity with IC_{50} values of 5.734 ± 1.365 and 5.319 ± 2.206 µg/mL, respectively, at the concentration tested. A plausible biogenetic pathway of the bisindole alkaloids has been proposed. Protein-ligand co-folding was used to generate protein-ligand complexes for the pfATP6 protein target and the isolated alkaloids. The stability of the modelled complexes was evaluated using molecular dynamics simulation. Scoring metrics of the generated complexes coupled to molecular mechanics generalized-born solvation rescoring of the modelled ligand poses were employed to explain the antimalarial structure-activity relationship for the investigated compounds. Alkaloids **2** and **3** can be considered as possible scaffolds for designing new antiplasmodial lead compounds.

1 | Introduction

The genus *Voacanga* belongs to the Apocynaceae and comprises about 14 different species. Amongst them, *Voacanga africana* Stapf Ex Scott-Elliot is the most cited species in the family. The traditional uses, biological activities, and toxicity profile of *V. africana* have been reported extensively [1–6]. *V. africana* is widely distributed in West Africa, Congo, Tanzania, and the Ivory Coast. The roots, leaves, and seeds of this plant species are used in African traditional medicine to treat malaria, leprosy, diarrhea, and other diseases [7–9]. Natural products isolated from *Voacanga* species have demonstrated anticancer, antimicrobial, anti-inflammatory, antibacterial, acetylcholinesterase, and other activities [10–17]. Previous phytochemical investigations have

shown the Apocynaceae plant to be rich in monoterpenoids and bisindole alkaloids [4, 6, 14, 18–23].

Recently, our group investigated the anti-*onchocercal* activity of alkaloids isolated from *V. africana* on both the microfilariae and adult male worms of *Onchocerca ochengi*. Eight alkaloids were found to possess activity against microfilariae but only moderate activity against adult worms. We carried out homology modeling, docking simulation, molecular dynamics (MD), and binding free energy calculations to explain the anti-*onchocercal* structure–activity relationship of the alkaloids [24]. Some of the alkaloids were found to inhibit the motility of both the microfilariae and adult male worms of *O. ochengi*, in a dose-dependent manner, but were only moderately active on the adult female worms upon biochemical assessment at 30 μM drug concentrations [24].

Bisindole alkaloids isolated from *Voacanga* species have shown interesting antimalarial activity against *Plasmodium falciparum* 3D7 [15], which warrants further investigation of the plant species. As part of our research effort directed at identifying bioactive compounds from African medicinal plants [24–26], the present study was aimed at evaluating the antimalarial activity of alkaloids isolated from *V. africana*. Herein, we report the isolation, structure elucidation, in vitro antiplasmodial activity, and molecular docking of an undescribed voacamine derivative, voacamine A (**1**), and the known alkaloids, voacamine (**2**), voacorine (**3**), and voacangine (**4**), with interesting yields. A plausible biogenetic pathway has been proposed for the isolated alkaloids. An attempt to explore the mode of action of these alkaloids and to explain the structure-activity relationship (SAR) led to deep learning-docking of the alkaloids and their corresponding fragments using the pfATP6 protein sequence. Since the reference compound artemisinin is known to bind to the drug target (pfATP6). The rationale was to attempt an initial SAR study by exploring the putative binding of these alkaloids to the target using fast in silico methods, then further suggest an in vitro study of the enzyme inhibition kinetics of these alkaloids against the target.

2 | Results and Discussion

2.1 | Purification and Characterization of the Alkaloids

Details on the isolation and identification of iboga-type alkaloids from the stem bark of *V. africana* methanol extract were previously reported by our group [24]. Voacamine A (**1**), voacamine (**2**), voacorine (**3**), and voacangine (**4**) were isolated as cream-colored solids and gave a positive reaction with Dragendorff's reagent. They were purified from the methanol extract of *V. africana* by successive chemical fractionation followed by purification through Sephadex LH-20 and preparative thin-layer chromatography (TLC). Their one- and two-dimensional nuclear magnetic resonance (1D and 2D NMR) spectra data (Figures S1–S15) showed the characteristics of iboga indole alkaloids when compared with published data in the literature. The alkaloids (Figure 1) were identified and characterized by comparison of experimental and reported spectroscopic data as voacamine A [27], voacamine [27, 28], voacorine [29], and voacangine, respectively [20, 22, 28].

Voacamine A (**1**) had ^{1}H and ^{13}C NMR data characteristic of a bisindole alkaloid (Table 1) [24]. All the chemical shifts of compound **1** were very similar to those of voacamine published in the literature [27]. Three important structural features could be confirmed by NMR, these included (i) the point of connection for the bisindole junction, (ii) the configuration of the ethyl chain at C-20', and (iii) the geometry of the ethylidene at C-20. The key Nuclear Overhauser Effect (A) and heteronuclear multiple bond coherence (B) correlations also confirm the structure of voacamine A (Figure 2). The Nuclear Overhauser Effect Spectroscopy (Figure S6) data show key structural differences between **1** and **2** [24].

2.2 | In Vitro Antimalarial Activity Evaluation of Alkaloids

Alkaloids **1–4** were subjected to in vitro antimalarial assays for their ability to inhibit the growth of asexual chloroquine-sensitive *P. falciparum* (*Pf*3D7). The bisindole alkaloids, voacamine (**2**) and voacorine (**3**), demonstrated good antiplasmodial profile with half-maximal inhibitory concentration (IC_{50}) values of 5.734 ± 1.365 and 5.319 ± 2.206 μg/mL, respectively, at the concentration tested (Table 2). This is not surprising, as previous studies have reported that bisindole alkaloids isolated from a phylogenetic species demonstrated potent antimalarial activity ($3.3 < IC_{50} < 5.3$ μM) against *P. falciparum* 3D7 [15]. Voacamine (**2**) was the most potent alkaloid and showed good in vitro *activity* against *P. falciparum* on both the D6 strain and chloroquine-resistant W2 strain [30]. The alkaloid has also demonstrated in vivo antiplasmodial activity. In synchronized cultures, voacamine (**2**) was found to act on trophozoite and schizont stages of *P. falciparum* [31]. The fact that voacamine A (**1**) was not active, while its isomer voacamine (**2**) had good activity, demonstrates the significance of stereochemical configurations on the observed biological properties.

2.3 | Proposed Plausible Biogenetic Pathway

The bisindole alkaloids isolated from *V. africana* are similar to the well-known vinblastine and vincristine isolated from *Catharanthus roseus* (Apocynaceae). Plants of the same family usually synthesize compounds of similar chemical classes due to the presence of structurally related enzymes that have similar biosynthetic pathways. These alkaloids are biosynthesised by the coupling of vobasinol (vobasinyl fragment) and voacangine (iboga fragment). To the best of our knowledge, the mechanism by which this coupling occurs in plants has not yet been elucidated extensively. Therefore, we propose the following plausible biogenetic pathway (Figure 3) to explain their formation. The biosynthesis of both fragments is known to proceed via the shikimic acid pathway, in which the precursor tryptophan is converted to tryptamine by tryptophan decarboxylase [32]. The mevalonic acid pathway forms loganin from geranyl pyrophosphate in a series of steps before its eventual conversion to secologanin by secologanin synthase [33]. Tryptamine and secologanin are then coupled by strictosidine synthase into strictosidine. Strictosidine is the main precursor of most monoterpene indole alkaloids. Therefore, vobasinol, voacangine, and voacristine are obtained from strictosidine. Coupling of these molecules or their

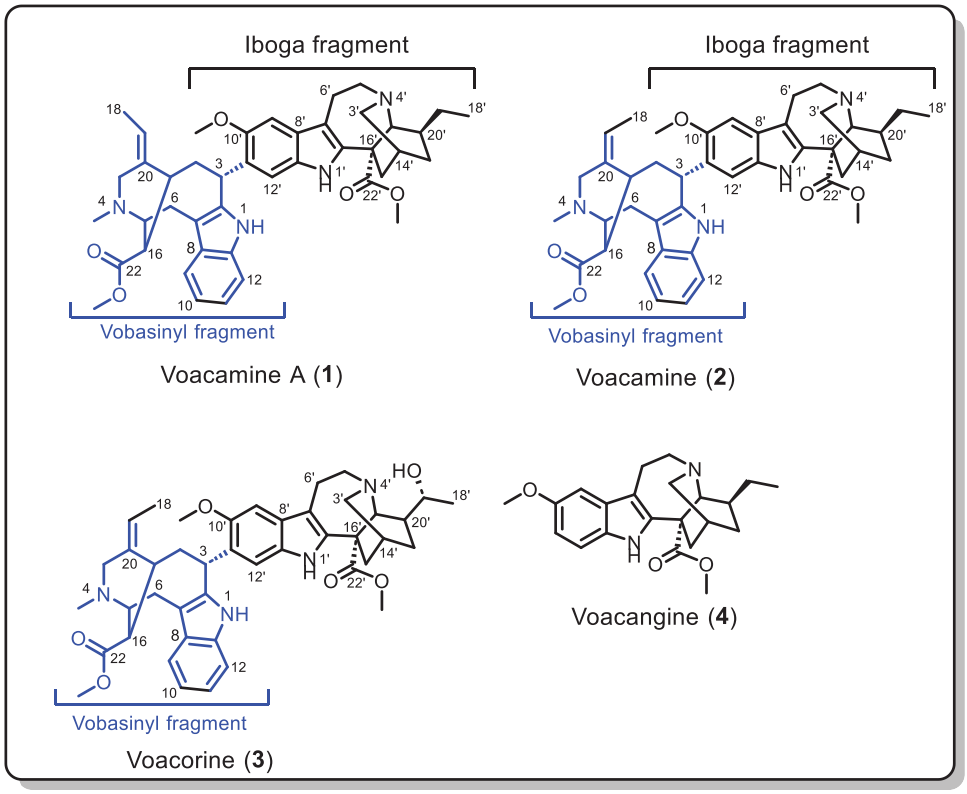

FIGURE 1 | Iboga-indole alkaloids isolated from *Voacanga africana*.

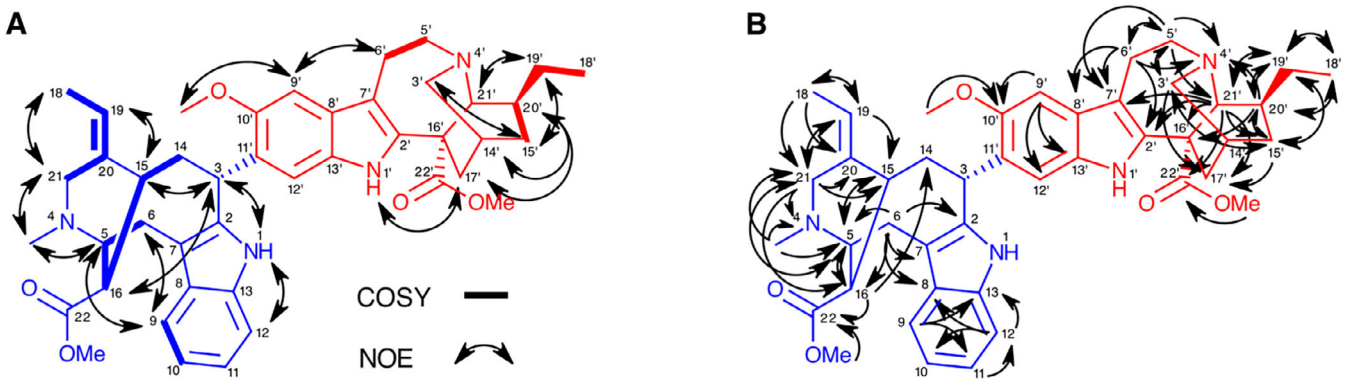

FIGURE 2 | Key nuclear Overhauser effect (NOE) (A) and heteronuclear multiple bond coherence (HMBC) (B) correlations in voacamine A [24].

precursors, facilitated by enzymes which are yet to be identified, leads to voacamine A (**1**), voacamine (**2**), and voacorine (**3**). The vobasinyl fragment of the coupled alkaloid rarely undergoes modifications after coupling, while the iboga fragment does [34]. If this hypothesis holds true, vobasinol may exist as two configurational isomers at the C-18′ vinyl methyl group: the *E* and *Z* configurations. The presence of both isomers could account for the formation of voacamine A (**1**). An alternative hypothesis posits that an electronically or conformationally excited state of vobasinol may undergo regioselective coupling, influenced by either electronic factors or the spatial orientation of neighboring substituents proximal to the C-18′ vinyl methyl group. A third possibility involves variation in the site of attachment of the iboga moiety to the vobasinol framework, analogous to the structural arrangement observed in ervachinines B and D [34]. However, detailed analysis of the NMR spectral data effectively rules out this option [24]. We therefore expect that the alkaloid voacamine A (**1**) will be reported from *Voacanga* or phylogenetic species in the near future.

3 | Molecular Docking Investigation

3.1 | Predicted Binding Pose Using Chai-1

Protein-ligand folding using the Chai-1 web server was employed to investigate the binding pose of the screened alkaloids to the parasite proteins. The pfATP6 protein target has multiple sites with the potential to harbour a ligand (Figure 4A). Chai-1 could fold the protein structures with acceptable confidence scores (PTM scores

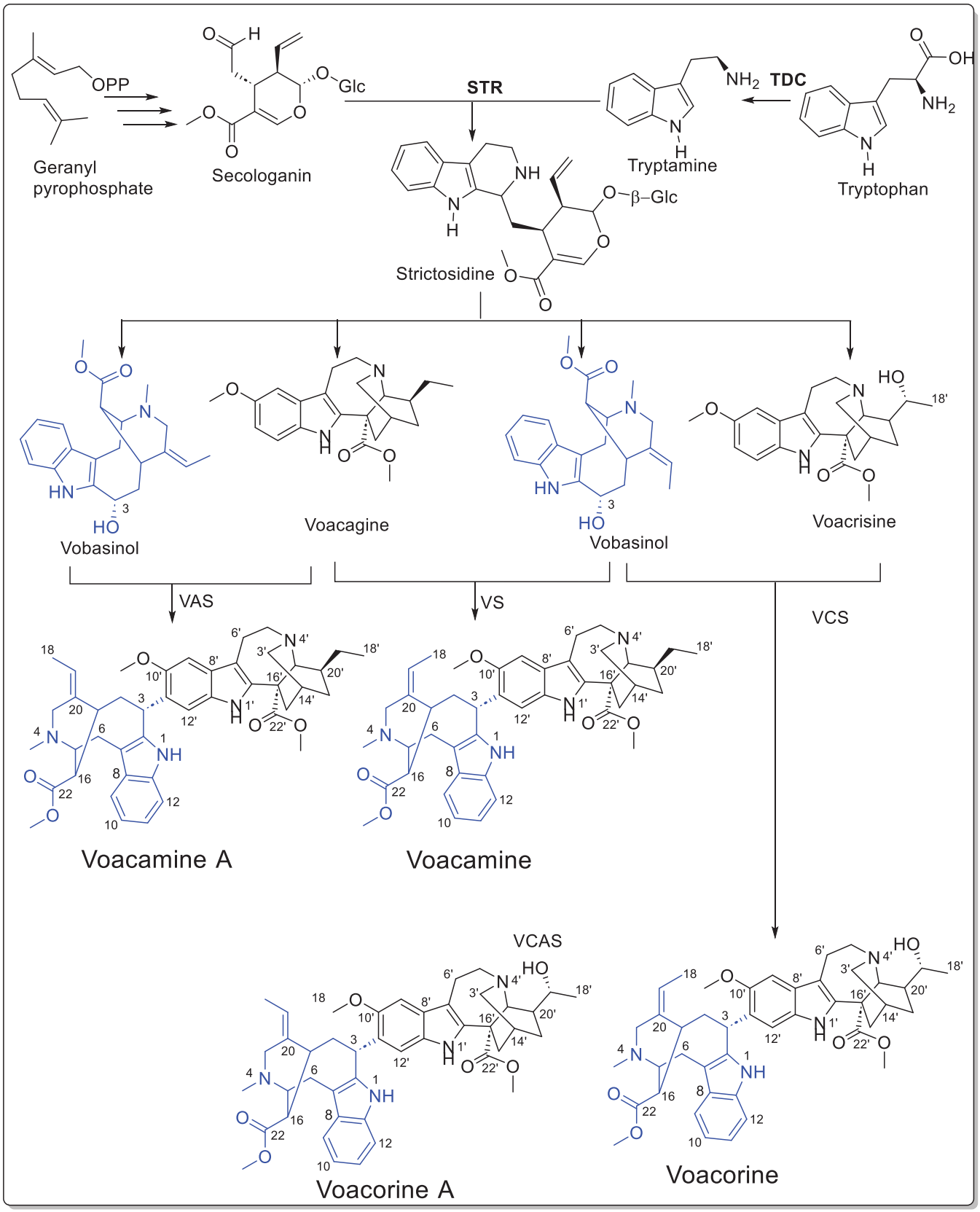

FIGURE 3 | Proposed plausible biogenetic pathway of voacamine, voacamine A, voacorine, and voacorine A. VAS: voacamine A synthase, VS: voacamine synthase, VCS: voacorine synthase, VCAS: voacorine A synthase [32–34].

TABLE 1 | Proton (^{1}H) (500 MHz) and carbon nuclear magnetic resonance (^{13}C NMR) (125 MHz) assignments for compound **1** in $CDCl_3$.

	1						
No.	δ_H	δ_C	δ_N	**No.**	δ_H	δ_C	δ_N
1	7.74 (1H)		127.2	1’	7.49 (1H)		120.1
2		137.3		2’		137.2	
3	5.17 (1H)	37.3		3’	2.89 (1H) 2.74 (1H)	51.9	
4			40.8	4’			20.3
5	4.07 (1H)	60.0		5’	3.40 (1H) 3.17 (1H)	53.1	
6	3.51 (1H) 3.28 (1H)	19.5		6’	3.12 (1H) 2.99 (1H)	22.2	
7		110.0		7’		110.0	
8		129.9		8’		127.4	
9	7.57 (1H)	117.4		9’	6.95 (1H, s)	99.2	
10	7.08 (1H)	119.0		10’		150.9	
11	7.07 (1H)	121.6		11’		129.8	
12	7.07 (1H)	109.8		12’	6.76 (1H)	110.3	
13		135.8		13’		130.3	
14	2.58 (1H) 2.02 (1H)	36.3		14’	1.82 (1H)	27.3	
15	3.80 (1H)	33.6		15’	1.70 (1H) 1.11 (1H)	32.0	
16	2.75 (1H)	47.0		16’		54.9	
17				17’	2.50 (1H) 1.78 (1H)	36.4	
18	1.69 (3H)	12.3		18’	0.90 (3H)	11.6	
19	5.36 (1H)	118.8		19’	1.56 (1H) 1.45 (1H)	26.7	
20		137.8		20’	1.31 (1H)	39.0	
21	3.76 (1H) 2.95 (1H)	52.6		21’	3.53 (1H)	57.2	
22 CO		171.5		22’ CO		175.3	
22 OMe	2.48 (3H)	49.9		22’ OMe	3.67 (3H)	52.4	
4 NMe	2.63 (3H)	42.4		10’ OMe	4.03 (3H)	56.1	

all > 0.8; Table 3; Table S1). The 3D surface-map representation of the modelled complexes reveals that the screened alkaloids all bind within the same pocket (Figure S16), which is similar to what was previously reported in the literature [35–38]. However, the confidence in placing the screened molecules to PfATP6 protein was low and did not correlate with the reported antimalarial activities (iPTM and Average_Ligand_all_atom_pLDDT scores < 0.6; Table S1).

Visual inspection of the predicted ligand pose showed consistent hydrophobic interaction patterns in the modelled structures of artemisinin and the isolated alkaloids (Figures 4B and 4C; Figure S16). For example, the biologically important peroxide bonds were exposed to the outside of the binding pocket. The structurally similar ligands, voacamine and voacamine A, presented varied outputs in the placement of the Iboga fragment. Nevertheless, this is not reflected in the key scoring metrics as the mean ligand atoms pLDDT scores and iPTM scores were the same for the top-ranked model (Table 3), thus indicating that the molecules might bind differently. This observed difference in pose can be used to explain the difference in observed antimalarial activity. Furthermore, the binding of the various moieties making up the respective molecules was predicted. The results show that the fragments were predicted with much higher confidence (almost 2-fold confidence). From their mean ligand atoms pLDDT scores and iPTM scores, we can suggest that the reported biological activity was mainly from the corresponding moieties (Iboga unit, vobasinyl, and voacristine), making the parent alkaloids.

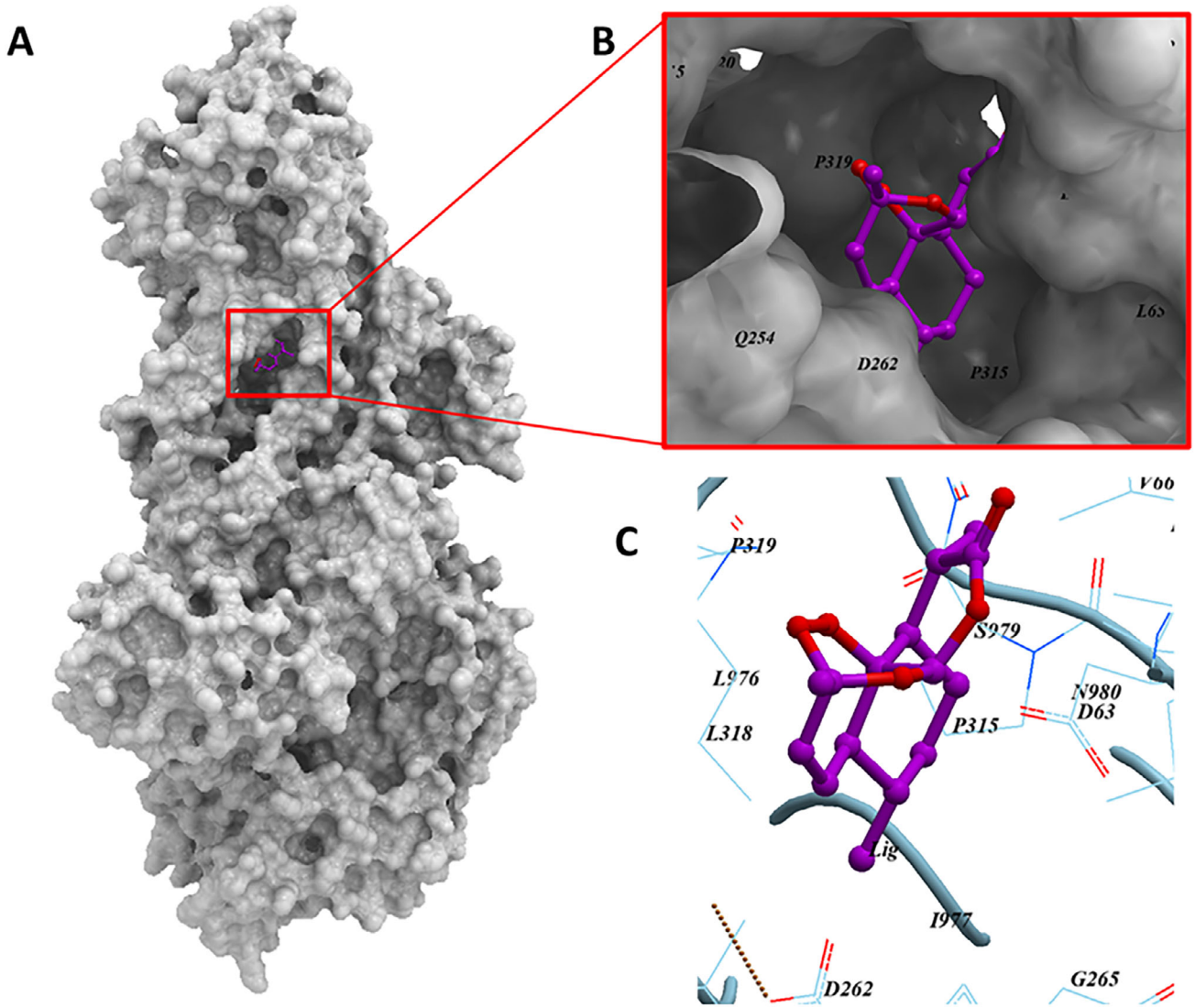

FIGURE 4 | Predicted pfATP6 protein/ligand complex. (A) Surface map of pfATP6 protein, (B) close view of the proposed cavity accommodating artemisinin, and (C) residues lining the binding site. The protein backbone is shown as a light blue ribbon, and residues are shown as lines. Artemisinin is depicted as purple balls and sticks.

TABLE 2 | In vitro inhibition of asexual stages of *P. falciparum* parasites.

Alkaloid	IC_{50} (μg/mL) ± SD
Voacamine A (**1**)	NA
Voacamine (**2**)	5.734 ± 1.365
Voacorine (**3**)	5.319 ± 2.206
Voacangine (**4**)	NA
Artemisinin	0.004 ± 0.001

NA = Not active, and IC_{50} is the concentration that inhibits 50% of the parasite maturation.

3.2 | Investigation of the Stability of the Modelled Structures

To investigate the reliability of the modelled structures in a close to biological situation, MD simulation is used to evaluate the stability of the protein–ligand structure. This is important because it considers the conditions in which pressure, temperature, and solvents correspond to the biological environment in the human body. The root mean square deviation (RMSD) plots help in measuring the difference between the ligand atoms from their starting structural conformation to their final position. Analysis of the data from MD simulation showed that some of the modelled structures, in particular, DihydroArtemisinin, Vobasinyl_fragment, and Voacristine exhibited desirable stability profiles as minimal deviation was observed throughout the simulation period for the protein and ligand (Figure 5A and Figure S17). Interestingly, the DihydroArtemisinin modelled structure had a better RMSD plot when compared to the Artemisinin. This confirms the fact that DihydroArtemisinin is the active form and shows how the dihydro group contributes to its stability. To the isolated compounds, A general trend was observed that the fragment molecules were more stable in the predicted binding site with RMSD around 1 Å and below. This correlates with the results from the Co-folding models presented in Table 3.

TABLE 3 | Summary of the top-ranked model for each protein-ligand complex.

Protein_ligand_model	Aggregate_score	ptm	iptm	Avg_Lig_pLDDT	Complex_pLDDT
pfATP6_Artemisinin_0	0.39	0.81	0.29	36.09	75.44
pfATP6_DihydroArtemisinin_0	0.44	0.81	0.34	47.33	75.53
pfATP6_Voacamine_0	0.47	0.81	0.38	47.69	75.32
pfATP6_Voacamine_A_0	0.47	0.81	0.38	47.55	75.39
pfATP6_Voacangine_0	0.59	0.82	0.53	70.06	75.58
pfATP6_Voacorine_0	0.46	0.81	0.38	44.49	75.33
pfATP6_Vobasinyl_fragment_0	0.63	0.82	0.58	72.78	75.83
pfATP6_Vobasinyl_fragment_a_0	0.57	0.82	0.50	78.24	75.88
pfATP6_voacristine_0	0.61	0.82	0.56	71.14	75.7

TABLE 4 | Summary of molecular mechanics generalized-born solvation (MM-GBSA) score (kJ/mol).

Compound	Recore_after_ Emin1	Recore_after_ Emin2	Recore_after_MD	Recore_after_ Emin3
Voacamine_A	−62.00	−63.76	−72.37	−83.76
Voacorine	−46.57	−66.71	−69.77	−81.22
Voacamine	−68.05	−69.72	−66.61	−60.98
Voacangine	−28.45	−36.17	−42.66	−47.39
Voacristine	−29.32	−36.96	−36.86	−39.36
Vobasinyl_fragment_A	−28.36	−31.88	−31.60	−37.68
Vobasinyl_fragment	−35.75	−38.30	−31.07	−36.77
Artemisinin	−20.18	−25.61	−29.92	−31.44
Dihydroartemisinin	−26.96	−33.60	−27.55	−28.83

3.3 | Rescoring of Modelled Structures Using Molecular Mechanics Generalized-Born Solvation

Rescoring of the modelled structures was equally done using the mbondi radii for the GB1 model from the AMBER package. The Tip3P solvation method and ion model were used. In this process, data generated from the MD Simulation step (trajectory file, parameter topology file) were used to score the molecules' interactions against their respective protein structure. Rescoring using this approach is very important because it takes into account the dynamics of the protein and solvation of the system. Summary data of the molecular mechanics generalized-born solvation (MM-GBSA) rescoring process are presented in Table 4. Although the rescoring was not perfect in ranking the molecules by the experimentally reported activity, it also confirmed that the fragment molecules (particularly, the Vobasinyl_fragment) were a major contributor to the activity.

4 | Conclusions

In this work, an undescribed bisindole alkaloid named voacamine A (**1**), along with the known alkaloids, voacamine (**2**), voacorine (**3**), and voacangine (**4**), were isolated from the stem barks of *V. africana*. The structures of the alkaloids were established by 1D and 2D NMR analyses. The bisindole alkaloids **2** and **3** showed a good in vitro antiplasmodial activity with IC_{50} values of 5.734 ± 1.365 and 5.319 ± 2.206 μg/mL, respectively, at the concentration tested. An attempt to explore the mode of action of these alkaloids and to explain the SAR led to DL-docking of all the alkaloids and their corresponding fragments using the pfATP6 protein sequence. Since the reference compound is known to bind to the aforementioned drug target, our rationale was to attempt an initial SAR study by exploring the putative binding of these alkaloids to the target in silico, then further suggest an in vitro study of the enzyme inhibition kinetics of these alkaloids against the target. Predicting the binding pose and the receptor site could explain the SARs of the isolated alkaloids in terms of reported metric scores. Further investigation to predict binding free energies towards the drug target site, complex stability, and interactions with site chain residues will be performed.

5 | Experimental

5.1 | General Experimental Procedures

Column chromatography was carried out with glass columns using Merck 60 (Merck, Darmstadt, Germany) (60–200 μm) silica gel as a stationary phase. Size exclusion chromatography was performed with Sephadex LH-20 (Sigma Aldrich, Seelze, Germany). Preparative TLC was performed using silica gel H. Analytical TLC

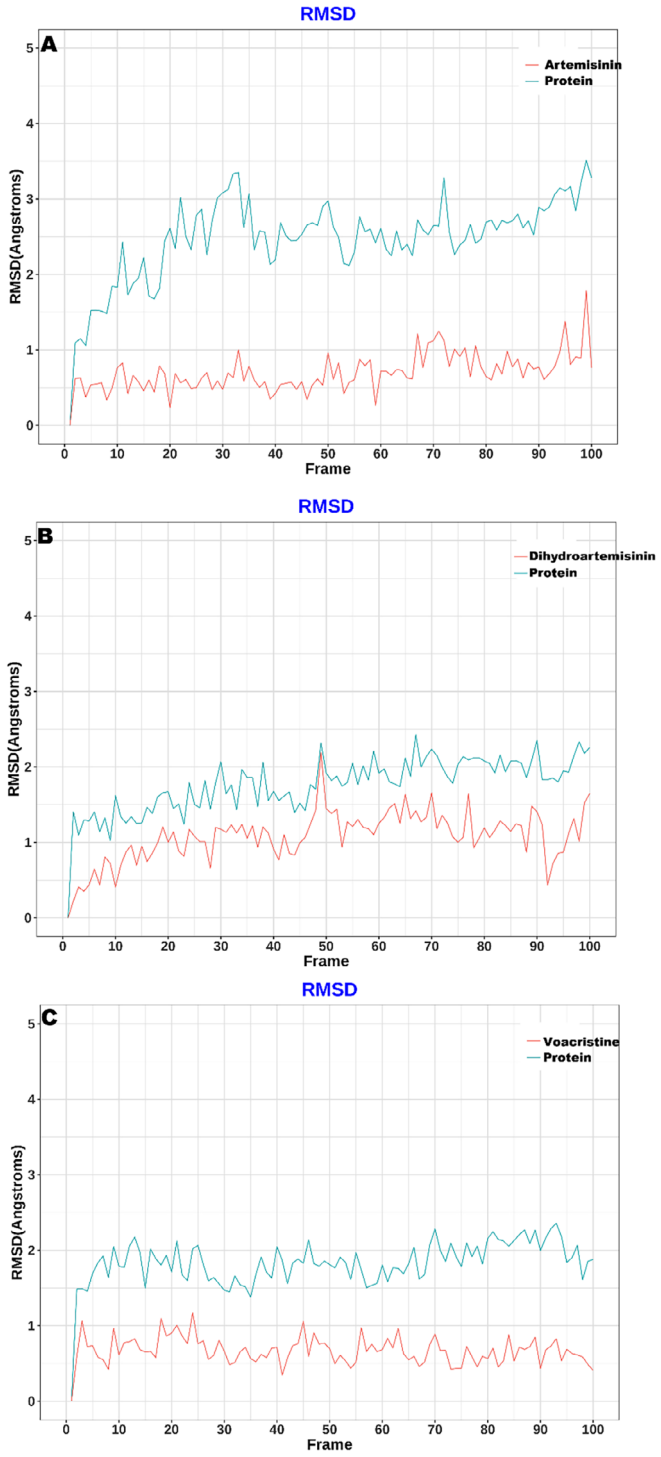

FIGURE 5 | Root mean square deviation (RMSD) plots for (A) artemisinin, (B) dihydrartemisinin, and (C) voacristine.

was performed on Merck F254 aluminum sheets precoated with silica gel. Zones on these plates were visualized under a UVGL-58 lamp (Analytica Jena, Upland, CA, USA) at 254/365 nm. Melting points were determined on a Mel Temp II apparatus (Merck, Darmstadt, Germany) and are uncorrected. Optical rotation was determined using an ADP430 digital polarimeter (Bellingham and Stanley, Tunbridge Wells, UK) at 20°C using the sodium D line (589 nm). Infrared (IR) spectroscopy was performed on a Spectrum 2 FT-IR spectrometer (PerkinElmer, Waltham, MA, USA) with a UATR accessory. Mass spectrometry was performed using a Xevo G2-S mass spectrometer (Waters, Elstree, UK) equipped with an atmospheric solids analysis probe, in positive ion mode. ^{1}H and ^{13}C NMR spectra were recorded in $CDCl_3$ at 500 and 125 MHz, respectively, with tetramethyl silane (TMS) as the internal reference, using an AVANCE III 500 MHz (^{1}H) NMR spectrometer equipped with a BBFO probe (Bruker, Billerica, MA, USA). The chemical shifts (*d*) of carbon and proton are in parts per million.

5.2 | Plant Material

The stem barks of *V. africana* Stapf (Apocynaceae) were collected in Ndop, Northwest Region of Cameroon. A voucher specimen of the plant, N°SCA887 was deposited at the Limbe Botanic Garden.

5.3 | Extraction and Isolation

The dried and powdered stem barks of *V. africana* (1.2 kg) were macerated in methanol at room temperature for nine days (3×3 days). Filtration and concentration of the crude extract on a rotary evaporator led to a dark greenish extract (25.5 g). Part of the crude extract (10.5 g) was subjected to silica gel normal phase open column chromatography and elution with a gradient of ethyl acetate in hexane. A total of 30 fractions were collected (250 mL each). The fractions were combined based on similar TLC profiles [silica 60 F254 gel-coated glass sheets with *n*-hexane and ethyl acetate to give five pooled fractions (A–E). Purifications through Sephadex LH-20, preparative TLC of C, and D yielded alkaloids **4** (90.6 mg), **1** (23.2 mg), **2** (34.2 mg), and **3** (17.2 mg), respectively.

6 | Characterization of alkaloids

6.1 | ^{13}C-NMR Data of the Alkaloids

Voacamine A (**1**): ^{13}C NMR ($CDCl_3$, 150 MHz), 175.3 (C-22), 171.5 (C-22), 150.9 (C-10′) 137.3 (C-2), 137.2 (C-1′), 130.3 (C-13′), 129.9 (C-8), 129.8 (C-11′), 127.4 (C-8′), 121.6 (C-11), 119.0 (C-10), 118.8 (C-19), 117.4 (C-9), 110.3 (C-12′), 110.0 (C-7′), 109.8 (C-12), 99.2 (C-9′), 60.0 (C-5), 57.2 (C-21′), 56.1 (10′-OMe), 54.9 (C-16′), 53.1 (C-5′), 52.4 (22′-OMe), 52.6 (C-21), 51.9 (C-3′), 49.9 (22-OMe), 47.0 (C-16), 42.4 (4-Me), 39.0 (C-20′), 37.3 (C-3), 36.3 (C-14), 36.4 (C-17′), 33.6 (C-15), 32.0 (C-15′), 27.3 (C-14′), 26.7 (C-19′), 22.2 (C-6′), 22.2 (C-6′), 19.5 (C-6), 12.3 (C-18), 11.6 (C-18′).

Voacamine (**2**): ^{13}C NMR ($CDCl_3$, 150 MHz), 173.7 (C-22′), 170.3 (C-22), 150.3 (C-10′) 139.0 (C-2), 137.2 (C-20), 136.1 (C-13), 130.5 (C-13′), 130.3 (C-8), 129.5 (C-11′), 126.4 (C-8′), 120.3 (C-11), 117.5 (C-10), 117.0 (C-19), 116.4 (C-9), 110.6 (C-12′), 110.0 (C-7′), 108.6 (C-12), 98.9 (C-9′), 59.4 (C-5), 57.0 (C-21′), 56.0 (10′-OMe), 54.4 (C-16′), 53.4 (C-5′), 52.1 (22′-OMe), 52.1 (C-21), 46.6 (C-16), 49.2 (C-16), 42.0 (4-Me), 39.0 (C-20′), 37.9 (C-9), 37.9 (C-3), 36.4 (C-14), 36.4 (C-17′), 33.4 (C-15), 32.0 (C-15′), 27.3 (C-14′), 26.7 (C-19′), 22.2 (C-6′), 19.4 (C-6), 12.3 (C-18), 11.6 (C-18′).

Voacorine (**3**): ^{13}C NMR ($CDCl_3$, 150 MHz), 175.2 (C-22′), 171.6 (C-22), 150.7 (C-10′) 143.1 (C-2′), 138.0 (C-2), 137.1 (C-20), 135.8 (C-13), 130.3 (C-13′), 129.9 (C-8), 129.8 (C-11′), 127.3 (C-8′), 121.5 (C-11), 118.8 (C-10), 118.5 (C-19), 117.4 (C-9), 110.3 (C-12′), 109.9 (C-7′),

109.8 (C-12), 99.2 (C-9′), 60.4 (C-5), 57.1 (C-21′), 56.1 (10′-OMe), 54.9 (C-16′), 53.1 (C-5′), 52.5 (22′-OMe), 52.4 (C-21), 49.9 (22-OMe), 47.0 (C-16), 42.4 (4-Me), 39.0 (C-20′), 37.4 (C-3), 36.4 (C-14), 36.4 (C-17′), 33.5 (C-15), 32.0 (C-15′), 27.3 (C-14′), 68.9 (C-19′), 22.2 (C-6′), 19.5 (C-6), 12.3 (C-18), 11.6 (C-18′).

Voacangine (**4**): ^{13}C NMR ($CDCl_3$, 150 MHz), $\underline{C}O_2Me$ (174.7), 153.0 (C-10), 136.5 (C-2), 130.5 (C-13), 129.2 (C-8), 111.8 (C-11), 111.1 (C-12), 110.1 (C-7), 100.8 (C-9), 57.5 (C-21), 56.0 (10-OMe), 55.1 (C-16), 53.1 (C-5), 52.4 ($CO_2\underline{Me}$), 51.5* (C-3), 39.1 (C-20), 35.5 (C-17), 32.0 (C-15), 27.4* (C-14), 26.7 (C-19), 21.2 (C-6), 11.6* (C-18).

7 | Biological Screening

7.1 | In Vitro Antimalarial Assay

The antiplasmodial test was assessed on a chloroquine-sensitive 3D7 *P. falciparum (Pf3D7)* strain, maintained in vitro as previously described in the literature with some modifications [39]. Parasites were maintained at 3% haematocrit (human type A red blood cells) in a complete culture medium (RPMI 1640 medium; Gibco, Fisher Scientific, Merelbeke, Belgium, containing $NaHCO_3$ (32 mM), HEPES (25 mM), and *L*-glutamine with 10% heat-inactivated human plasma, 1.76 g/L of glucose; Sigma-Aldrich, Overijse, Belgium, 44 mg/mL of hypoxanthine; Sigma-Aldrich, Overijse, Belgium, and 100 mg/L of gentamicin; Gibco, Fisher Scientific, Merelbeke, Belgium). All cultures were placed in a humidified incubator at 37 °C with a standard gas mixture of 5% O_2, 5% CO_2, and 90% N_2. Parasitaemia was verified by microscopy using Giemsa-stained thin films. A stock solution of compounds and artemisinin (used as a standard) was prepared by dissolving 5 mg in 1 mL DMSO and diluting it with culture media. The anti-plasmodial test was performed at an initial concentration of 25 and 1 µg/mL (compounds and artemisinin, respectively) and serially diluted to eight concentrations. Each sample was tested in duplicate wells with the parasites at a final volume of 250 µL (DMSO < 1%). Wells with parasites only served as the positive control, while the negative control consisted of wells with culture medium only. After 48 h of incubation, parasite growth was estimated by the determination of plasmodial lactate dehydrogenase activity [40]. The IC_{50} values were calculated by linear regression. All tests were repeated at least twice.

8 | Molecular Docking Studies

8.1 | Prediction of Binding Pose and Analysis of Modelled Structures

The 1228 amino acid sequence of the *P*-type calcium transporting ATPase for *P. falciparum* (PfATP6) was obtained from https://www.uniprot.org/uniprotkb/E5RU00/entry (accessed February 21, 2025). To model the selected complexes, a Chai-1 server was used (https://lab.chaidiscovery.com/dashboard; accessed February 21–24, 2025). For the modelling of each complex structure, the protein amino acid sequence and the corresponding ligand SMILES were used as the inputs for Chai-1. The default settings included the use of MMseqs2 for multiple sequence alignment, restraints, and no template in the modelling. For each input, Chai-1 outputs five modelled structures, and the selected "best structure" for our analysis was based on the aggregate_score generated by Chai-1. Analysis and comparison of the different modelled complexes were done using ipTM, ptm, average_complex pLDDT and average_ligand_atoms pLDDT.

8.2 | MD Simulation

The modelled structures from Chai-1 were subjected to a 100 ns MD simulation using AMBER software version 20 [41]. The antechamber module of AMBER was used to parameterise and correct the bond order of the small molecules. The Tleap module was used to prepare and generate the MD system for each modelled structure. In this process, each system was neutralised with counterions and solvated using the TIP3P solvation model in an octahedral box with 10 Å from the protein [42].

The prepared systems were used to run MD simulation, and the process involved the following steps; 1) a two-step minimization of 4000 iterations (consisting of 3000 steepest descents followed by a 1000 conjugate gradients) were the ligand and protein were fixed to their initial coordinates using a force constant of 10 kcal mol^{-1} Å^{-1} to remove steric clashes between the solvent molecules and ions used to neutralize the system. 2) A second minimization of 4000 iterations (consisting of 2000 steepest descent followed by 2000 conjugate gradient) involving the whole system (solvent, ions, protein, and ligand) was performed. 3) Heating of the systems from 0 to 300 K through 100 ps while restraining the atoms of the protein and ligand (with a force constant of 10 kcal mol^{-1} Å^{-1}) to prevent large structural deviation. 4) 100 ps evaluation of Density. 6) Equilibration of the systems through a 5 ns MD simulation, and finally, the proper 100 ns MD simulation production step. Throughout, the SHAKE algorithm was used to restrain all bonds involving hydrogens, while the temperature of the different systems was controlled by Langevin Dynamics, using a collision frequency of 2 ps^{-1} and a pressure of 1 bar. The MD simulation trajectories were analyzed using the CPPTRAJ module of the AMBER software [43].

8.3 | Rescoring With MM-GBSA

The MMPBSA.py script for MM-GB/Poisson-Boltzmann Surface Area (MM-GB/PBSA) PB/GBSA implemented in AMBER was used to re-score the modelled structures [41]. This Python script estimates the corresponding BFE for each complex, creating an ensemble average of both the receptor and the ligand after the removal of appropriate atoms in each complex. All estimates are made from the parameter-topology file, which contains all the information required by the various energy functions, as well as being specific to each molecular system, and is also directly related to the coordinate file.

Acknowledgments

The research was funded by the Alexander von Humboldt Foundation for Georg Forster and Georg Forster-Bayer Research fellowships (Ref. 3.4–CMR–1220727–GF-P) at the University of Tübingen, Germany.

Conflicts of Interest

The authors declare no conflicts of interest.

Data Availability Statement

The data that support the findings of this study are available in the Supporting Information of this article. Physical samples of the alkaloids may be requested from the corresponding authors.

References

1. P. W. Grosvenor, P. K. Gothard, N. C. Mc William, A. Supriono, and D. O. Gray, "Medicinal Plants from Riau Province, Sumatra, Indonesia. Part 1: Uses," *Journal of Ethnopharmacology* 45 (1995): 75–95, https://doi.org/10.1016/0378-8741(94)01209-I.

2. P. A. G. M. De Smet, "Some Ethnopharmacological Notes on African Hallucinogens," *Journal of Ethnopharmacology* 50 (1996): 141–146, https://doi.org/10.1016/0378-8741(95)01337-7.

3. S. B. Kombian, T. M. Saleh, N. I. Y. Fiagbe, et al., "Ibogaine and a Total Alkaloidal Extract of Voacanga africana Modulate Neuronal Excitability and Synaptic Transmission in the Rat Parabrachial Nucleus In Vitro," *Brain Research Bulletin* 44, no. 5 (1997): 603–610, https://doi.org/10.1016/s0361-9230(97)00284-0.

4. A. P. G. Macabeo, G. J. D. Alejandro, A. V. Hallare, W. S. Vidar, and O. B. Villaflores, "Phytochemical Survey and Pharmacological Activities of the Indole Alkaloids in the Genus Voacanga Thouars (Apocynaceae) – An Update," *Pharmacognosy Reviews* 3 (2009): 132–142, www.phcogrev.com.

5. H. Hussain, J. Hussain, A. Al-Harrasi, and I. R. Green, "Chemistry and Biology of the Genus Voacanga," *Pharmaceutical Biology* 50 (2012): 1183–1193, https://doi.org/10.3109/13880209.2012.658478.

6. E. O. Bekoe, J. A. A. Opare, M. Lartey, and P. Amoateng, "Ethnomedicinal Uses, Biological Activities, and Toxicity of Voacanga africana Stapf Ex Scott-Elliot," *Advances in Traditional Medicine* 24 (2024): 431–448, https://doi.org/10.1007/s13596-023-00709-y.

7. P. V. Tan and B. Nyasse, "Anti-ulcer Compound from Voacanga africana with Possible Histamine H2 Receptor Blocking Activity," *Phytomedicine* 7 (2000): 509–515, https://doi.org/10.1016/S0944-7113(00)80037-9.

8. P. V. Tan, V. B. Penlap, B. Nyasse, and J. D. B. Nguemo, "Anti-ulcer Actions of the Bark Methanol Extract of Voacanga africana in Different Experimental Ulcer Models in Rats," *Journal of Ethnopharmacology* 73 (2000): 423–428, https://doi.org/10.1016/S0378-8741(00)00292-0.

9. H. Terashima and M. A. Ichikawa, "A Comparative Ethnobotany of the Mbuti and Efe Hunter-Gatherers in the Ituri Forest, Democratic Republic of Congo," *African Study Monographs* 24, no. 1,2 (2003): 1–168, https://doi.org/10.14989/68220.

10. R. Kikura-Hanajiri, T. Maruyama, A. Miyashita, and Y. Goda, "Research into the Component Analysis and DNA Analysis of the Plant-Based Illegal Drug Voacanga africana," *Yakugaku Zasshi* 129, (2009): 975–982, https://doi.org/10.1248/yakushi.129.975.

11. M. Kitajima, M. Iwai, R. Kikura-Hanajiri, et al., "Discovery of Indole Alkaloids with Cannabinoid CB1 Receptor Antagonistic Activity," *Bioorganic & Medicinal Chemistry* 21 (2011): 1962–1964, https://doi.org/10.1016/j.bmcl.2011.02.036.

12. S. B. Babiaka, J. Mbah, F. Cho-Ngwa, J. Metuge, and S. Efange, "Isolation and Characterization of Filaricidal Compounds from the Stem Bark of Voacanga africana, a Plant Used in the Traditional Treatment of Onchocerciasis in Cameroon," *Journal of Medicinal Plants Research* 9, no. 14 (2015): 471–478, https://doi.org/10.5897/jmpr2014.5791.

13. Y. Niu, C. Yang, J. Zhou, S. Huang, and J. Liu, "Two New Compounds with Antimicrobial Activities from the Seeds of Voacanga africana," *Phytochemistry Letters* 18 (2016): 208–212, https://doi.org/10.1016/j.phytol.2016.10.019.

14. A. Dey, A. Mukherjee, and M. Chaudhury, "Chapter 10 - Alkaloids from Apocynaceae: Origin, Pharmacotherapeutic Properties, and Structure-Activity Studies," *Studies in Natural Products Chemistry* 52 (2017): 373–487, https://doi.org/10.1016/B978-0-444-63931-8.00010-2.

15. A. E. Nugroho, Y. Ono, E. Jin, et al., "Bisindole Alkaloids from Voacanga grandifolia Leaves," *Journal of Natural Medicines* 75 (2021): 408–414, https://doi.org/10.1007/s11418-020-01475-w.

16. H. Fouotsa, P. Le Pogam, P. Mkounga, et al., "Voatriafricanines A and B, Trimeric Vobasine-Aspidosperma-Aspidosperma Alkaloids from Voacanga africana," *Journal of Natural Products* 84 (2021): 2755–2761, https://doi.org/10.1021/acs.jnatprod.1c00812.

17. J. A. H. Manzano, E. A. Abellanosa, J. P. Aguilar, et al., "Globospiramine from Voacanga globosa Exerts Robust Cytotoxic and Antiproliferative Activities on Cancer Cells by Inducing Caspase-Dependent Apoptosis in A549 Cells and Inhibiting MAPK14 (p38α): In Vitro and Computational Investigations," *Cells* 13 (2024): 772, https://doi.org/10.3390/cells13090772.

18. K. V. Rao, "Alkaloids of Voacanga Africana, Stapf. I. Voacafrine and Voacafricine-Two New Alkaloids," *Journal of Organic Chemistry* 23 (1958): 1455–1456.

19. D. W. Thomas and K. Biemann, "The Hydroxyindolenine Derivative of Voacangine, a New Indole Alkaloid from Voacanga africana," *Tetrahedron* 24 (1987): 4223–4231, https://doi.org/10.1016/0040-4020(68)88184-0.

20. H. M. Chen, Y. T. Yang, H. X. Li, et al., "Cytotoxic Monoterpenoid Indole Alkaloids Isolated from the Barks of Voacanga africana Staph," *Natural Product Research* 30 (2016): 1144–1149, https://doi.org/10.1080/14786419.2015.1046132.

21. M. Kitajima and H. Takayama, "Monoterpenoid Bisindole Alkaloids," *Alkaloids: Chemistry and Biology* 76 (2016): 259–310, https://doi.org/10.1016/bs.alkal.2015.09.001.

22. M. Harada, K. N. Asaba, M. Iwai, N. Kogure, M. Kitajima, and H. Takayama, "Asymmetric Total Synthesis of an Iboga-Type Indole Alkaloid, Voacangalactone, NewlyIsolated from Voacanga africana," *Organic Letters* 14 (2012): 5800–5803, https://doi.org/10.1021/ol3027945.

23. Q. Zhao, W. T. Zhu, X. Ding, et al., "Voacafrines A-N, Aspidosperma-Type Monoterpenoid Indole Alkaloids from Voacanga africana with AChE Inhibitory Activity," *Phytochemistry* 181 (2021): 112566, https://doi.org/10.1016/j.phytochem.2020.112566.

24. S. B. Babiaka, C. V. Simoben, K. O. Abuga, et al., "Alkaloids with Anti-Onchocercal Activity from Voacanga africana Stapf (Apocynaceae): Identification and Molecular Modeling," *Molecules* 26 (2021): 70, https://doi.org/10.3390/molecules26010070.

25. S. B. Babiaka, R. Nia, K. O. Abuga, et al., "Antioxidant Potential of Flavonoid Glycosides from Manniophyton fulvum Müll. (Euphorbiaceae): Identification and Molecular Modeling," *Scientific African* 8 (2020): e00423, https://doi.org/10.1016/j.sciaf.2020.e00423.

26. C. E. Nkwelle, S. B. Babiaka, C. S. Metuge, et al., "Croton oligandrus Pierre & Hutch (Euphorbiaceae) Extracts and Isolated Compounds Reverse HIV-1 Latency," *Journal of Experimental Pharmacology* (2024): 413–425, https://doi.org/10.2147/JEP.S472234.

27. W. L. B. Medeiros, I. J. C. Vieira, L. Mathias, et al., "Two known Bis-Indole Alkaloids Isolated from Tabernaemontana laeta: Complete ^{1}H and ^{13}C Chemical Shift Assignments," *Magnetic Resonance in Chemistry* 37 (1999): 676–681, https://doi.org/10.1002/(SICI)1097-458X(199909)37:9⟨676.

28. J. P. Kutney, A. Horinaka, R. S. Ward, and B. R. Worth, "Studies on the Total Synthesis of Bisindole Alkaloids Within the Voacamine Family," *Canadian Journal of Chemistry* 58 (1980): 1829–1838, https://doi.org/10.1139/V80-288.

29. G. Buchi, R. E. Manning, and S. A. Monti, "Voacamine and Voacorine," *Journal of the American Chemical Society* 86 (1964): 4631–4641, https://doi.org/10.1021/ja01075a02.

30. E. Federici, G. Palazzino, C. Galef, and M. Nicoletti, "Antiplasmodial Activity of the Alkaloids of Peschiera fuchsiaefolia," *Planta Medica* 66, no. 1 (2000): 93–95, https://doi.org/10.1055/s-0029-1243122, https://www.ncbi.nlm.nih.gov/pubmed/10705750.

31. D. Ramanitrahasimbola, P. Rasoanaivo, S. Ratsimamanga-Urverg, et al., "Biological Activities of the Plant-Derived Bisindole Voacamine

with Reference to Malaria," *Phytotherapy Research* 15 (2001): 30–33, https://doi.org/10.1002/1099-1573(200102)15.

32. S. A. Bradley, B. J. Lehka, F. G. Hansson, et al., "Biosynthesis of Natural and Halogenated Plant Monoterpene Indole Alkaloids in Yeast" *Nature Chemical Biology* 19 (2023): 1551–1560, https://doi.org/10.1038/s41589-023-01430-2.

33. Q. M. Dudley, S. Jo, D. A. S. Guerrero, et al., "Reconstitution of Monoterpene Indole Alkaloid Biosynthesis in Genome Engineered Nicotiana benthamiana," *Communications Biology* 5 (2022): 949, https://doi.org/10.1038/s42003-022-03904-w.

34. C. Lavaud and G. Massiot, "The Iboga Alkaloids," in *Progress in the Chemistry of Organic Natural Products 105 Chem Org Nat Prod*, eds. A.D. Kinghorn, H. Falk, S. Gibbons, and J. Kobayashi. (Springer International Publishing AG, 2017), 89–136, https://doi.org/10.1007/978-3-319-49712-9_2.

35. M. Jung, H. Kim, K. Y. Nam, and K. T. No, "Three-Dimensional Structure of Plasmodium falciparum Ca^{2+}-ATPase(PfATP6) and Docking of Artemisinin Derivatives to PfATP6," *Bioorganic & Medicinal Chemistry Letters* 15, no. 12 (2005): 2994–2997, https://doi.org/10.1016/j.bmcl.2005.04.041.

36. P. K. Naik, M. Srivastava, P. Bajaj, et al., "The Binding Modes and Binding Affinities of Artemisinin Derivatives with Plasmodium falciparum Ca^{2+}-ATPase (PfATP6)," *Journal of Molecular Modeling* 17 (2011): 333–357, https://doi.org/10.1007/s00894-010-0726-4.

37. C. M. Moore, J. Wang, Q. Lin, et al., "Selective Inhibition of Plasmodium falciparum ATPase 6 by Artemisinins and Identification of New Classes of Inhibitors after Expression in Yeast," *Antimicrobial Agents and Chemotherapy* 66, no. 5 (2022): e02079-21, https://doi.org/10.1128/aac.02079-21.

38. I. Tsamesidis, F. Mousavizadeh, C. O. Egwu, et al., "In Vitro and In Silico Antimalarial Evaluation of FM-AZ, a New Artemisinin Derivative," *Medicines* 9, no. 2 (2022): 8, https://doi.org/10.3390/medicines9020008.

39. W. Trager and J. B. Jensen, "Human Malaria Parasites in Continuous Culture," *Science* 193, no. 4254 (1976): 673–675, https://doi.org/10.1126/SCIENCE.781840.

40. M. Kenmogne, E. Prost, D. Harakat, et al., "Five Labdane Diterpenoids from the Seeds of Aframomum zambesiacum," *Phytochemistry* 67 (2006): 433–438, https://doi.org/10.1016/j.phytochem.2005.10.015.

41. D. A. Case, K. Belfon, I. Y. Ben-Shalom, et al. *AMBER*. University of California (2020).

42. W. L. Jorgensen, J. Chandrasekhar, J. D. Madura, R. W. Impey, and M. L. Klein, "Comparison of Simple Potential Functions for Simulating Liquid Water," *Journal of Chemical Physics* 79 (1983): 926, https://doi.org/10.1063/1.445869.

43. D. R. Roe and T. E. Cheatham, "PTRAJ and CPPTRAJ: Software for Processing and Analysis of Molecular Dynamics Trajectory Data," *Journal of Chemical Theory and Computation* 9 (2013): 3084, https://doi.org/10.1021/ct400341p.

Supporting Information

Additional supporting information can be found online in the Supporting Information section.

Supporting File 1: cbdv70564-sup-0001-SuppMat.docx **Supporting File 2**: cbdv70564-sup-0002-FigureS16.png **Supporting File 3**: cbdv70564-sup-0003-FigureS17.png